ACCSCIENCE PUBLISHING

Journal of Seismic Exploration

ARTICLE

A novel method for low-frequency quality control of seismic vibrator ground force

Mingtao Nie[1,2], Zhouhong Wei[3]*, Tao Fang[2], Xiaolong Jiang[2], Yongan Xu[2], Yang Liu[1], and Yongfei Qi[1,2]

[1]State Key Laboratory of Petroleum Resources and Engineering, China University of Petroleum (Beijing), Beijing, China

[2]BGP, China National Petroleum Corporation, Zhuozhou, Hebei, China

[3]INOVA Geophysical, Sugar Land, Texas, United States

Abstract

Seismic vibrators are the primary sources for land seismic acquisition, featuring controllable bandwidth and energy, low environmental impact, safety, and high efficiency. With the widespread application of "2W&H" technology, wide-frequency seismic data, particularly low-frequency components, have attracted increasing attention. However, the ground force output of a vibrator is severely constrained at low frequencies, primarily due to limitations in its mechanical and hydraulic systems. Among these, hydraulic system limitations are often associated with oil flow, which is largely constrained by the pump's maximum capacity; however, oil flow is not measured during vibrator sweeps. The system complexity prevents the installation of flow sensors on vibrators, making the performance of the vibrator oil flow unmonitored. Since the oil flow directly determines the quality of the vibrator ground force output, it is essential to understand the behavior of vibrator oil flow. In this study, a detailed analysis of the working mechanism of a seismic vibrator was conducted, as well as its low-frequency force-output limitations. Then, we proposed a method for estimating vibrator oil flow. Both theoretical analyses and field-testing data were used to validate the proposed estimation method. The estimated data demonstrated strong consistency with the direct flow measurement using flow sensors. Moreover, the results confirm the feasibility of the proposed estimation method. This method provides a real-time quality control indicator for the vibrator oil flow performance during vibrator sweeps, thereby enabling complete monitoring of the vibrator performance quality at low frequencies. In addition, this method holds promising potential for broad application in land vibroseis exploration.

Keywords: Vibrator; Low-frequency; Oil flow; Quality control

***Corresponding author:**
Zhouhong Wei
(John.Wei@inovageo.com)

Citation: Nie M, Wei Z, Fang T, *et al*. A novel method for low-frequency quality control of seismic vibrator ground force. *J Seismic Explor*. 2026;35(1):171-183. doi: 10.36922/JSE025410086

Received: October 11, 2025

Revised: November 10, 2025

Accepted: December 10, 2025

Published online: January 15, 2026

1. Introduction

Hydraulic seismic vibrators have been used as the primary source for land seismic surveys for over 60 years. Over the years, many innovative vibroseis acquisition techniques have been developed, leading to significant improvements in acquisition productivity. For example, Rozemond[1] introduced a slip-sweep acquisition method, and the high-fidelity vibratory-seismic method was developed by Allen *et al.*[2] In addition, the

distance separated simultaneous source was developed and presented by Bouska,[3] and a more flexible simultaneous source acquisition technique, independent simultaneous source acquisition, was invented by Howe *et al.*[4]

Recently, vibroseis low-frequency acquisition has become a routine practice in land seismic surveys. Seismic vibrator manufacturers have been making progress in vibrator actuator design to improve vibrator low-frequency performance.[5-10] However, these improvements still cannot meet the force spectrum required at low frequencies. To acquire more low-frequency data, the use of custom nonlinear sweep signals based on low-dwell technology has become a routine operation in land seismic surveys.[11-14] However, how to perform quality control (QC) of seismic vibrator performance at low frequencies remains a challenge. In geophysics literature, few studies have been devoted to seismic vibrator QC at low frequencies. Moreover, apart from the study by Sallas,[15] very few technical papers have provided a concise explanation of how a hydraulic seismic vibrator works, particularly regarding the hydraulic power supply system.

In the present study, we first present a detailed introduction to how a hydraulic seismic vibrator works. Then, we discuss the limitations experienced by a seismic vibrator when it operates at low frequencies. The reaction mass displacement limitation is physically measured and monitored in the vibrator field QC. However, the other limitation—vibrator oil flow—is not physically measured or monitored in QC. Next, considerable effort is devoted to the study of vibrator oil flow, and a novel method is proposed for estimating vibrator oil flow to enable QC of the low-frequency ground force. Finally, we conduct experimental tests to assess the agreement between the estimated and measured oil flow. Consequently, field QC of vibrator oil flow becomes possible.

2. Theoretical analysis

2.1. Challenges from low-frequency acquisition

In field operation, low-dwell sweeps must be used on seismic vibrators to push the vibroseis acquisition bandwidth toward the low end of the spectrum. These low-dwell sweeps typically shake seismic vibrators at low frequencies for extended periods of time to boost low-frequency force-energy. Seismic vibrators often work at the edge of their maximal capabilities, especially in the seismic vibrator hydraulic system. Fatigue, wear, and failure become inevitable in vibrator system components. Consequently, the quality of the vibrator ground force is affected, thereby reducing the quality of seismic data. For example, in 2021, a crew in the Middle East desert experienced a total failure of seven pilot servo-valves and severe damage to vibrator pumps in only 2 weeks of operation.

Figure 1 presents an example illustrating the consequences of this field operation when the hydraulic pump flow limitation is reached. Figure 1A shows the frequency–time (F–T) variant spectrum of the vibrator ground force. In the ground-force signal, a very strong spike appears when the sweep changes from a nonlinear sweep rate to a linear sweep rate. This indicates that severe cavitation possibly occurs in the vibrator pump system. Figure 1B shows strong harmonic noise associated with severe cavitation observed on the shot record; the cavitation can lead to severe damage to the vibrator pump. Figure 1C displays severe scratches observed on the port plate of the hydraulic pump.

These findings demonstrate that, when the vibrator operates at low frequencies, the hydraulic flow limitation is reached. In addition, the vibrator ground force is contaminated with spiky noise, leading to additional harmonic noise in seismic records and damage to hydraulic system components. This results in a significant reduction in the production rate. In addition, repairing these pilot servo-valves and hydraulic pumps significantly increases operating costs. Hence, it is necessary to monitor the seismic vibrator motion and performance at low frequencies so that early warnings can be triggered before the vibrator system components fail completely.

2.2. Vibrator hydraulic working principle

Figure 2 illustrates how a hydraulic seismic vibrator works. A seismic vibrator is essentially a hydro-mechanical system driven by a servo-valve assembly controlled electronically. The vibrator system consists of two subsystems—the vibrator hydraulic power supply system and the vibrator actuator system—connected through a pressurized oil flow. The vibrator hydraulic power supply system generates the required high-pressure oil flow for the vibrator actuator system. The output shaft of a diesel engine is connected to the pump shaft so that the engine's rotational power can be transferred to the pump.

A variable displacement pressure piston pump, through a high-pressure adjustment device, produces a high-pressure oil flow and outputs it into hoses. The pressurized oil flow goes through a high-pressure filter to remove particles and impurities from the oil circuit. Filtering these impurities effectively prevents severe cavitation in the oil flow circuit. After filtration, the filtered oil flow passes through a high-pressure accumulator. The main function of the high-pressure accumulator is to suppress pressure fluctuations and maintain the high pressure at a constant level (3,250 psi). At this point, the high-pressure oil flow is

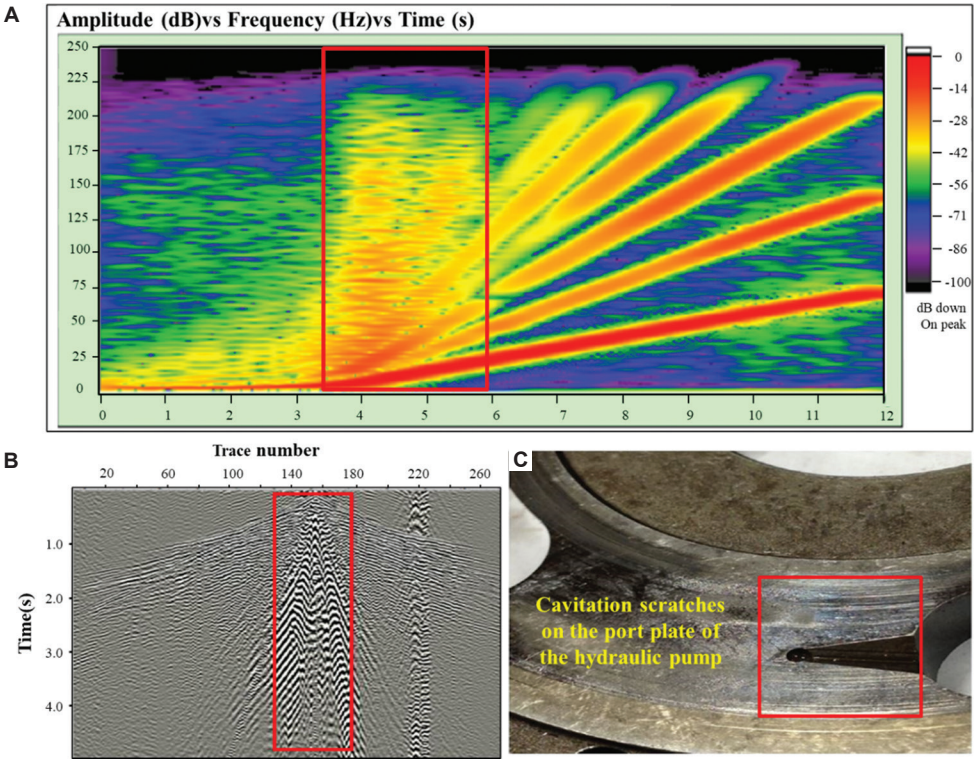

Figure 1. Examples of hydraulic flow limitation in a seismic vibrator. (A) Frequency–time variant spectrum of the vibrator ground force, illustrating a strong spiky noise (red box). (B) Seismic record displaying harmonic noise (red box) caused by the spiky ground force. (C) Mechanical damage observed on the hydraulic pump caused by the spiky ground force.

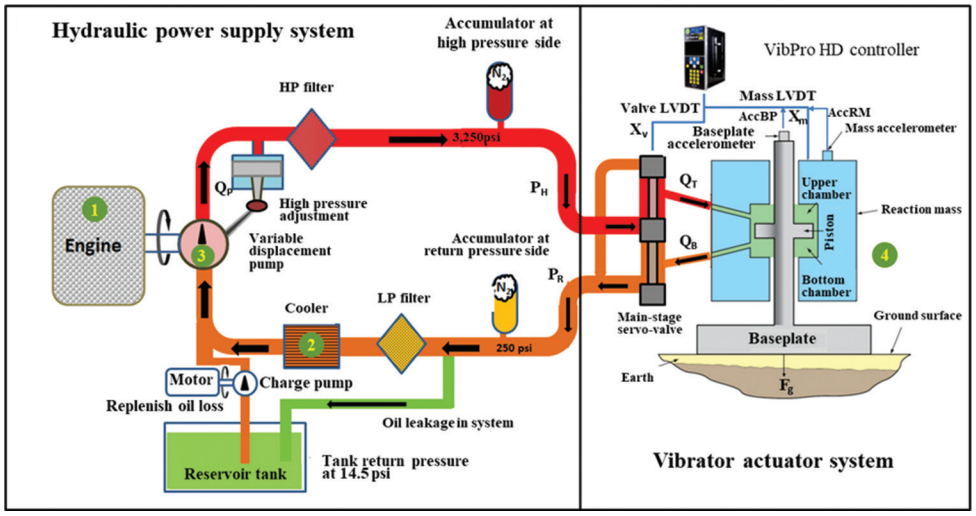

Figure 2. Schematic illustration of a hydraulic seismic vibrator
Abbreviations: AccBP: Accelerations of baseplate; AccRM: Accelerations of reaction mass; LP: Low pressure; LVDT: Linear variable differential transformer.

ready to leave the hydraulic power supply system and enter the vibrator actuator system.

The high-pressure fluid flows into the main-stage servo-valve. The displacement of the main-stage servo-valve is controlled by a vibrator controller. Specifically, the Vib Pro HD controller regulates the displacement of the main-stage servo-valve. In fact, it controls the current of the pilot servo-valve (not depicted in the diagram). The electrical current of the pilot servo-valve is proportional to the displacement of the main-stage servo-valve. For

simplicity, we assume that the vibrator controller directly controls the displacement of the main-stage servo-valve.

The high-pressure hydraulic fluid output from a control port of the main-stage servo-valve, Q_T, flows into the upper chamber of the reaction mass, rapidly increasing the pressure in the upper chamber. This increased pressure pushes the reaction mass upward. At the same time, the same pressure is applied to the top surface of the piston, causing the piston to move downward, resulting in a downward movement of the vibrator baseplate. Furthermore, the upward movement of the reaction mass and the downward movement of the baseplate combine to form a weighted-sum ground force (F_g), which is then transmitted into the deep ground.[16]

When the high-pressure oil fluid flows into the upper chamber of the reaction mass, the reaction mass moves upward, increasing the volume of the upper chamber while reducing the volume of the bottom chamber. The hydraulic oil fluid, Q_B, flows out of the bottom chamber and returns to the low-pressure side, or return side, of the hydraulic power supply system through another control port of the main-stage servo-valve. The oil flow leaves the vibrator actuator system and returns to the hydraulic power supply system. It also passes through a low-pressure accumulator to reduce pressure ripples and stabilize the return pressure. Typically, the return-side pressure is maintained at 250 psi. The return flow also passes through a low-pressure filter for filtration. The filtered low-pressure hydraulic oil then goes through a cooling system to dissipate heat. The cooled hydraulic oil is subsequently drawn into the pump again, and a new cycle begins.

During vibrator operation, some hydraulic oil loss is inevitable due to internal and external leakages in the hydraulic system. Therefore, a special hydraulic circuit is designed and added to allow the leaked oil fluid to flow back to a reservoir tank, effectively preventing environmental contamination. In addition, a small charge pump is added to the hydraulic circuit to compensate for the loss of hydraulic oil in the hydraulic system. As noted, in the vibrator system, hydraulic oil flow is an essential element that transfers energy, converting hydraulic energy into mechanical motion and ground force output.

2.3. Low-frequency limitations

In recent years, low-frequency vibroseis acquisition has become a routine practice in land seismic exploration.[17] Through years of field practice, field experience, and analysis have shown that the seismic vibrator ground force at low frequencies is severely limited due to constraints in the vibrator's mechanical and hydraulic systems. Wei[18] and Sallas[19] have studied the seismic vibrator extensively, concluding that the ground force at low frequencies is mainly limited by two key factors: the maximal travel distance of the reaction mass, also referred to as the mass stroke limit, and the vibrator's total flow, which is primarily determined by the hydraulic pumps (pump flow limit).[20]

Specifically, regarding the maximal travel distance of the reaction mass, **Equation 1** expresses the relationship between the maximal low-frequency ground force and the maximal reaction mass displacement, as well as the mass of the reaction mass.

$$F_{max1} = 4\pi^2 M_{rm} X_{rm} f^2 \tag{1}$$

Where F_{max1} is the maximum force that can be theoretically generated by the vibrator mechanical system at low frequencies, M_{rm} is the mass of the reaction mass, X_{rm} is the maximum travel distance of the reaction mass, and f is the frequency. Based on **Equation 1**, there is no parameter related to the vibrator hydraulic system. Thus, **Equation 1** expresses the low-frequency ground force limitation solely from the vibrator mechanical system.

Equation 2 provides an expression based solely on the vibrator hydraulic system. For a given vibrator, the hydraulically limited low-frequency force scales with the available total flow.

$$F_{max2} = 9.87 \frac{M_{rm} Q}{A_p} f \tag{2}$$

Where F_{max2} is the maximum force that can be theoretically generated by the vibrator oil flow at low frequencies, A_p is the piston area in the reaction mass chambers, and Q is the maximum vibrator oil flow, primarily contributed by the vibrator pump flow.

In summary, the vibrator ground force at low frequencies is determined by the reaction mass stroke for a given vibrator (**Equation 1**) and is also constrained by the vibrator's total flow (**Equation 2**). Given the specifications of a vibrator, a low-frequency force profile can be calculated using **Equations 1** and **2**.

Table 1 lists the key specifications of AHV-IV 364 (60,000-lbf) and AHV-IV 380 (80,000-lbf) vibrators. Using these specifications, their low-frequency force profiles can be obtained. Figure 3 shows the theoretical low-frequency force profiles for the AHV-IV 364 and AHV-IV 380 vibrators. The force curves at low frequencies (<10 Hz) were plotted using **Equations 1** and **2** with the specifications listed in Table 1. It can be clearly seen that the vibrator force curves at low frequencies are limited parabolically by the maximal reaction mass displacement and linearly by the vibrator total flow.

Table 1. Specifications of AHV-IV vibrators

Parameters	AHV-IV 364 vibrator	AHV-IV 380 vibrator
Peak force (lbs)	61,800	77,700
Reaction-mass weight (*Mrm*; lbs)	11,020	13,029
Peak-to-peak useful mass stroke (*Xrm*; in)	3.87	3.87
Pumps (*Qp*; gallon/min)	Two P7; 164 gallon/min	Two P8; 187 gallon/min
Piston area (Ap; in^2)	20.67	25.92

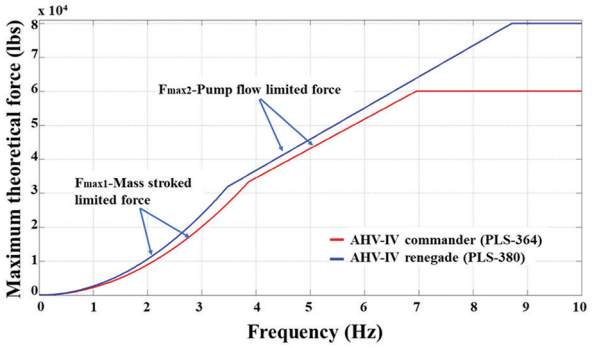

Figure 3. Theoretical low-frequency force profiles of AHV-IV vibrators

To overcome these limitations on the seismic vibrator ground force at low frequencies, several researchers, especially from vibrator manufacturers, have attempted to redesign the vibrator hydraulic and mechanical systems so that the vibrator mechanical system becomes more rigid and the hydraulic power supply system becomes more efficient and less noisy.[7,19-21] Field testing results have shown that at low frequencies, notable improvements in the vibrator ground force and reductions in harmonic distortion are observed. A remarkable improvement in the signal-to-noise ratio of the vibrator ground force is achieved. Thus, an extension of the vibroseis acquisition frequency bandwidth toward 1.5 Hz becomes achievable. However, these force improvements are still insufficient to meet the required force-energy in the frequency range below 5 Hz.

To meet the required force-energy, the low-dwell sweep is necessary. Several researchers[21-24] have explored different approaches, including low-frequency sweep design techniques, to supply extra force-energy so that the vibroseis acquisition bandwidth can be extended toward low frequencies (<5 Hz). These low-frequency sweep techniques aim to guide seismic vibrators to follow as closely as possible their low-frequency force profiles. Qi *et al.*[13] demonstrate how a low-frequency sweep is designed for a given mode of vibrator.

To date, with the most advanced vibrator technologies, combining the latest low-frequency seismic vibrator with customized low-dwell sweeps, the low-frequency vibroseis acquisition bandwidth has been extended to record seismic data as low as 1.5 Hz.[7] A good acquisition production rate is also achieved. However, challenges remain in preventing the complete failure of vibrator system components during vibroseis field operations. In other words, performing QC on seismic vibrator performance at low frequencies remains very challenging.

To address the limitation of the vibrator mechanical system, a reaction mass linear variable differential transformer (LVDT) sensor is mounted on the reaction mass to measure the reaction mass displacement in real-time. An LVDT is a type of sensor used for high-accuracy position or displacement measurements. Thus, the reaction-mass travel distance during a sweep becomes a known variable, and its real-time measurements are recorded in a vibrator QC report, for example, an extended QC text file.

Figure 4 illustrates the results of QC of the reaction-mass displacement. It can be clearly seen that the reaction-mass displacement between 3.5 s and 4.5 s, corresponding to frequencies from 3 Hz to 6 Hz, reaches its maximal stroke limit. For modern seismic vibrator control electronics, a limit control is embedded to prevent the vibrator reaction mass from reaching its maximal displacement limitation.

However, the vibrator oil flow or pump flow—a limitation of the vibrator hydraulic system—is not measured, as there is no flow sensor installed on seismic vibrators. Therefore, the status of the vibrator oil flow becomes a "black box." The vibrator flow status across the entire sweep bandwidth remains unknown, particularly in the low-frequency range. System reliability and complexity prevent the installation of flow sensors. Nonetheless, during a sweep, it is essential to understand how to obtain vibrator oil flow information. Thus, it is important to investigate the theoretical behavior of vibrator flow and develop a method to estimate the vibrator oil flow.

2.4. Theory: Total flow going to the reaction mass chamber

As shown in Figure 2, when the flow is output from the main-stage servo-valve, it goes to the reaction mass chamber (e.g., upper chamber). The vibrator oil flow in the reaction mass chamber follows the governing equation:

$$Q = V_{rm} A_p \tag{3}$$

Where Q denotes the total flow going to the reaction mass chamber; V_{rm} represents the reaction mass velocity—a relative velocity between the reaction mass and the baseplate; A_p is the piston area in the reaction mass chambers.

Based on **Equation 3**, the vibrator oil flow can be estimated using the relative velocity of the reaction mass and the baseplate. The reaction mass and baseplate accelerations are measured in real-time for every vibrator sweep in field production. Hence, the relative velocity can be obtained by integrating the measured accelerations.

Figure 5A displays the measured reaction-mass and baseplate accelerations, where an AHV-IV 362 (60,000-lbf) vibrator performs a linear sweep from 1 to 21 Hz over a duration of 10 s, with a 1-s long cosine taper at the front end of the sweep on regular soil. This vibrator is equipped with two P7 pumps, and the maximal flow delivered by the two pumps is 167 gallons/min.

To evaluate the accuracy of the estimation algorithms, two accelerations are recorded with a sampling time interval of 0.25 ms, corresponding to a sampling frequency of 4,000 Hz. To obtain the relative velocity of the reaction mass, the accelerations are preprocessed to remove direct-current offsets, followed by application of a low-bandpass filter. Two acceleration curves shown in Figure 5A have had their direct-current offsets and high-frequency noise removed.

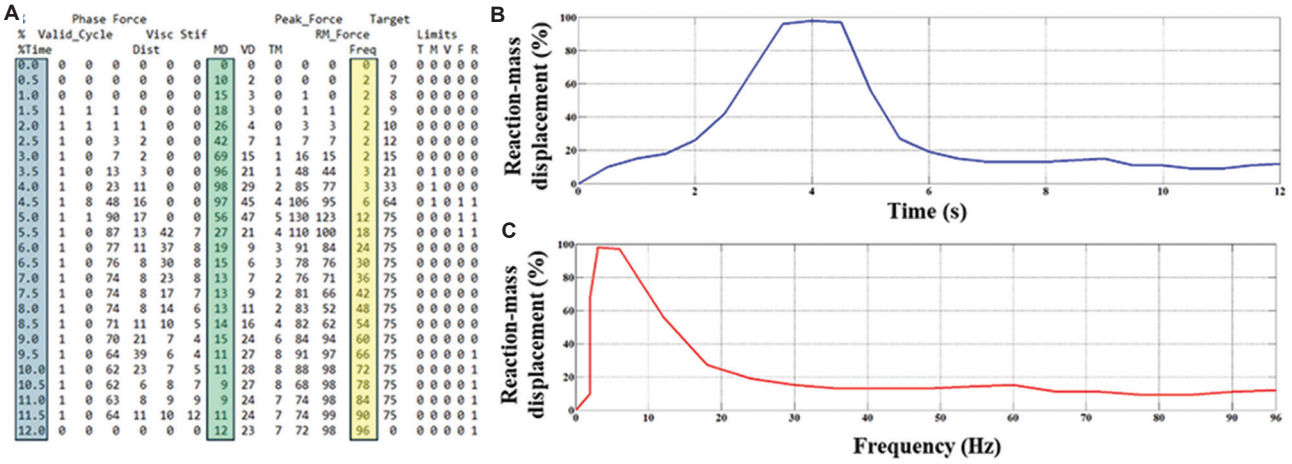

Figure 4. Reaction-mass displacement quality control. (A) Extended vibrator quality control data, with the blue bar indicating the sweep time series at 500 ms intervals, the yellow bar representing the corresponding frequencies of the first column, and the green bar showing the reaction-mass displacement during the sweep. (B) Reaction-mass displacement quality control data in the time domain. (C) Reaction-mass displacement quality control data in the frequency domain.

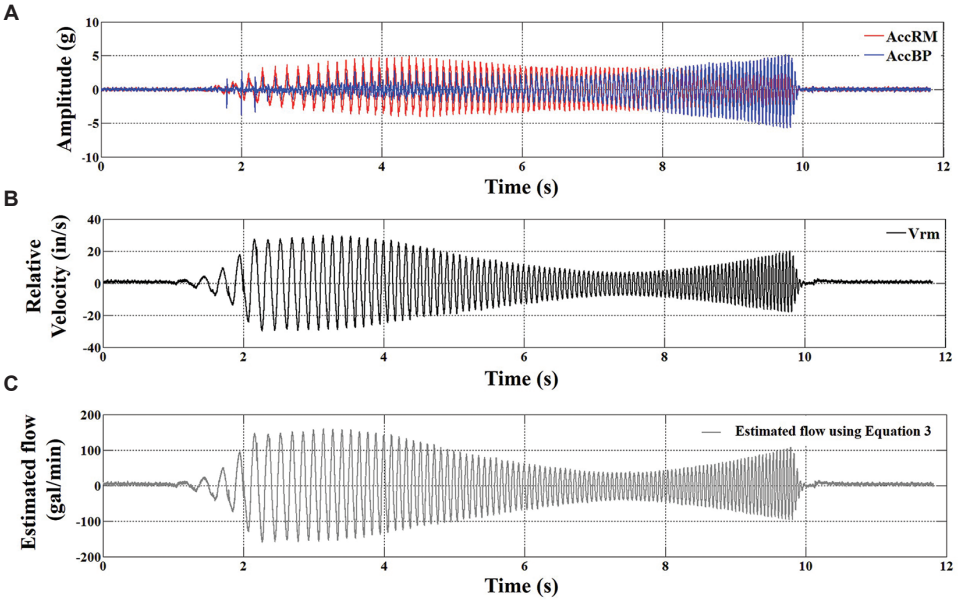

Figure 5. Signal display of (A) measured reaction-mass and baseplate accelerations on an AHV-IV 362 vibrator; (B) calculated reaction-mass velocity; and (C) estimated vibrator oil flow using **Equation 3**

After preprocessing, an integration operation is applied to both the reaction mass and baseplate acceleration. As a result, the relative velocity between the reaction mass and the baseplate is computed (Figure 5B). Finally, the vibrator oil flow is estimated using **Equation 3** and is plotted (Figure 5C).

It can be observed that the estimated vibrator oil flow remains at approximately 150 gallons/min between 2s and 4s, corresponding to the frequency range from 5 Hz to 9 Hz. During this time interval, the vibrator oil flow closely approaches the vibrator flow limitation of 167 gallons/min. In other words, the estimated vibrator flow curve indicates that the vibrator oil flow reaches approximately 90% of the hydraulic system's maximum flow capacity. This curve serves as an indicator and suggests that the vibrator hydraulic system components may be operating under potentially harmful vibration conditions. At this point, the question becomes, "How do we know whether the estimation using **Equation 3** is reasonable?" In practice, direct flow measurement is not available because flow sensors are not installed on the seismic vibrator, due to system complexity and extensive hardware modifications required for installation. Consequently, direct flow measurement is unrealistic in real vibroseis acquisition. Nevertheless, an alternative method based on the main-stage servo-valve can be used to calculate the vibrator oil flow. This method is presented in this study as an indirect validation of the estimation approach derived from **Equation 3**.

3. Solution and verification

3.1. Main-stage servo-valve total flow verification

As illustrated in Figure 2, the vibrator oil flow going to the reaction-mass upper chamber is equivalent to the flow output from the main-stage servo-valve. A modern seismic vibrator actuator is driven by a hydraulic servo-valve assembly consisting of a Moog 760-928A pilot servo-valve and an Atlas 240H main-stage servo-valve. When supported by vibrator control electronics (e.g., Vib Pro HD controllers), an optional Pelton DR-valve can be installed between the pilot servo-valve and the main-stage servo-valve.

Figure 6 shows an example of a servo-valve assembly mounted on a modern seismic vibrator. The main-stage servo-valve, specifically the Atlas 240H, alternately outputs oil flow to drive the seismic vibrator actuator. The governing equation for the servo-valve flow is expressed in **Equation 4**. Merritt[25] is a valuable source, offering comprehensive knowledge and a thorough treatment of servo-valve technology.[25] The governing equation is as follows:

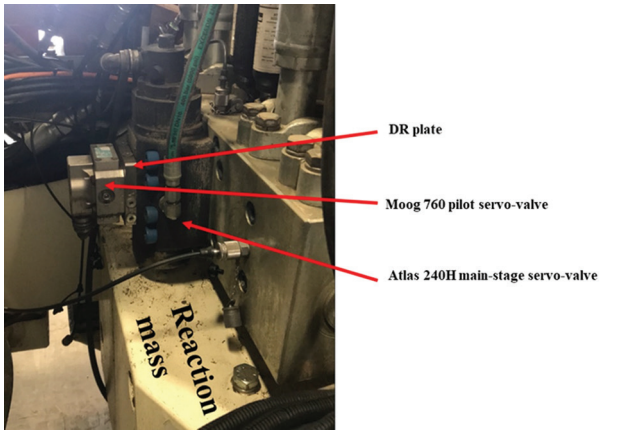

Figure 6. Servo-valve assembly installed on a modern seismic vibrator

$$Q = Kx_v\sqrt{P_s - \frac{x_v}{|x_v|}P_d} \quad \text{(IV)}$$

Where:

(i) Q denotes the total flow output from the main-stage servo-valve control ports A and B (in^3/s).

(ii) K is the flow–pressure coefficient ($in^2/s/\sqrt{psi}$).

(iii) x_v represents the displacement of the main-stage servo-valve (in).

(iv) P_s is the supply pressure to the main-stage servo-valve (psi).

(v) P_d represents the differential pressure across control ports A and B of the main-stage servo-valve (psi).

The supply pressure is equivalent to the system high pressure minus the system return pressure. Typically, the system high pressure is set at 3,250 psi, and the system return pressure is set at 250 psi. Thus, the supply pressure is 3,000 psi. The hydraulic oil flow is delivered through the main-stage servo-valve control ports, resulting in a differential pressure across control ports A and B on the main-stage servo-valve. This differential pressure theoretically corresponds to the differential pressure across the piston in the reaction-mass chamber. By controlling the displacement of the main-stage servo-valve spool, the differential pressure across the piston can therefore be controlled.

Based on **Equation 4**, the oil flow from the main-stage servo-valve, Q, can be estimated if the supply pressure, the displacement of the main-stage servo-valve, and the differential pressure across the piston in the reaction-mass chamber are known. To estimate the vibrator flow using **Equation 4**, four pressure sensors were installed on the main-stage servo-valve of the AHV-IV 362 vibrator to measure the system high pressure, system return pressure, and the differential pressure at control A and B,

respectively. During the tests, a Vib Pro controller drove the vibrator with a linear sweep from 1 to 21 Hz over 10 s at a 70% force level (42,000 lbs). The sweep rate was 2 Hz/s, the start taper was 1 s, and the end taper was 0.2 s.

Figure 7 illustrates the supply pressure measurements, illustrating the system high pressure and system return pressure. In general, the high pressure remains around 3,250 psi, and the return pressure remains at 250 psi. Pressure ripples or spikes are observed on the high- and return-pressure signals.

The pressure fluctuation is more pronounced in the supply pressure. Figure 8 presents the differential pressure measurements, illustrating the pressures measured at control ports A and B. The differential pressure was calculated as the pressure measured at control port A minus the pressure measured at control port B. Since the main-stage servo-valve is equipped with an LVDT transducer to measure its displacement for servo-valve feedback position control, the displacement of the main-stage servo-valve was measured and recorded by the vibrator controller in real time. Figure 9 displays the measured displacement of the main-stage servo-valve during this sweep.

By incorporating all measurements into **Equation 4**, where the flow-pressure coefficient (K) was set to 292, the total vibrator oil flow was estimated for this sweep.

Figure 10A illustrates the estimated flow responses using **Equations 3** and **4**. In general, it can be seen that the flow curves show a strong similarity. To better demonstrate the similarity between the two flow curves, a similarity line was constructed using the x–y coordinates and is

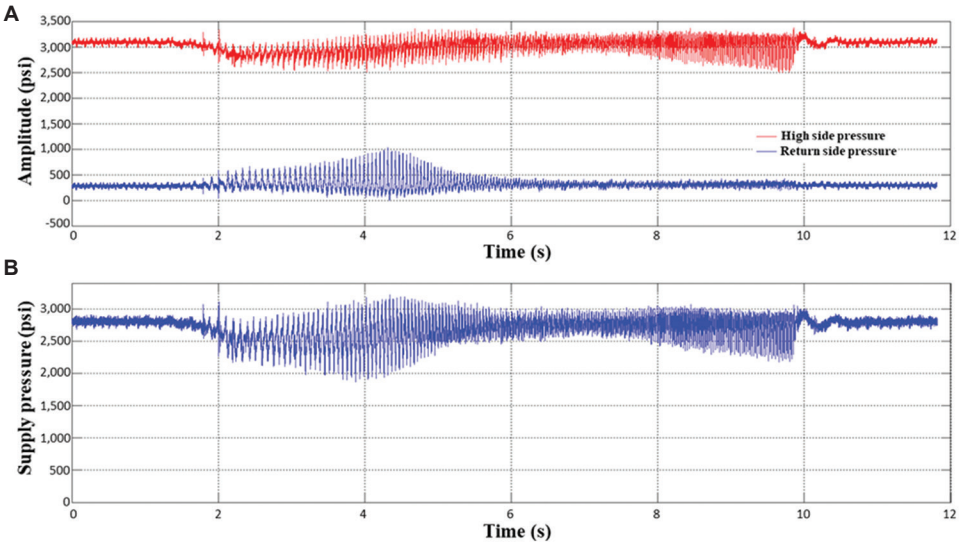

Figure 7. Measured system high pressure and system return pressure on an AHV-IV 362 vibrator

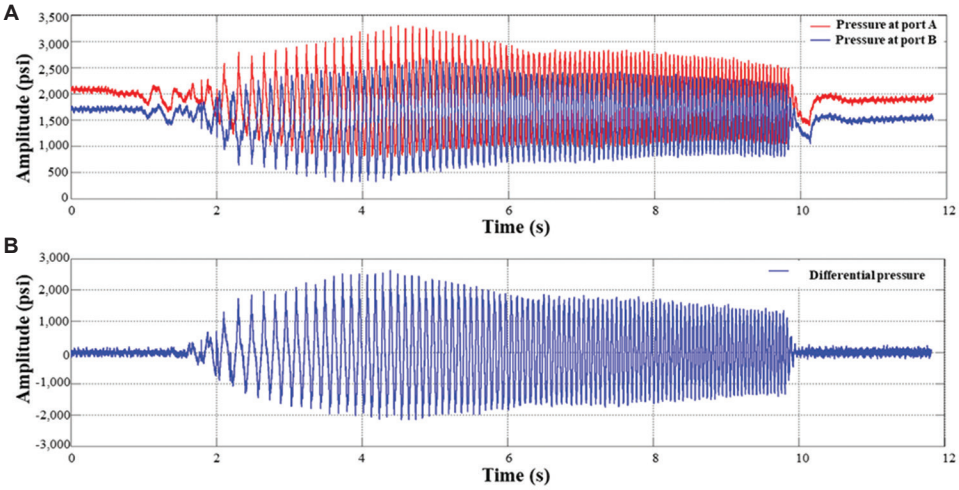

Figure 8. Measured differential pressure at control ports A and B on an AHV-IV 362 vibrator

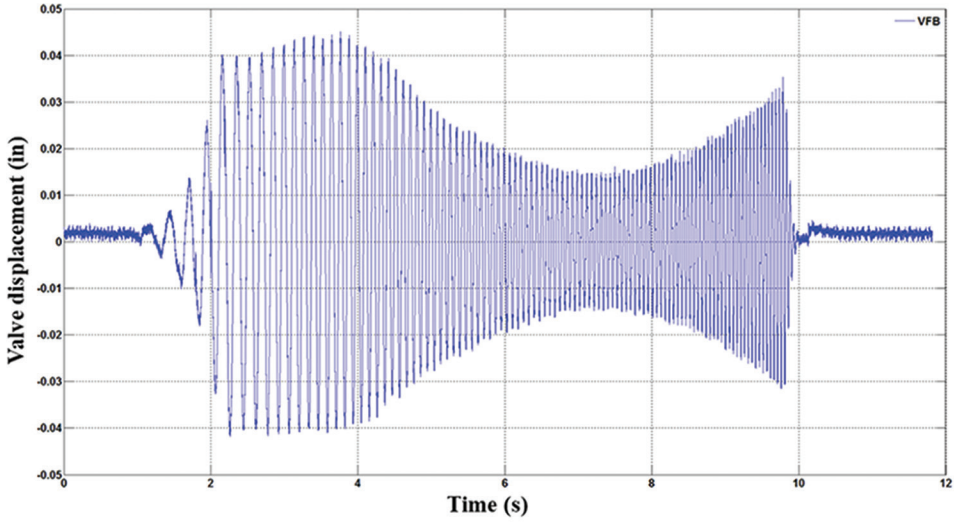

Figure 9. Measured displacement of the Atlas 240 H main-stage servo-valve on an AHV-IV 362 vibrator
Abbreviations: VFB: Valve feedback.

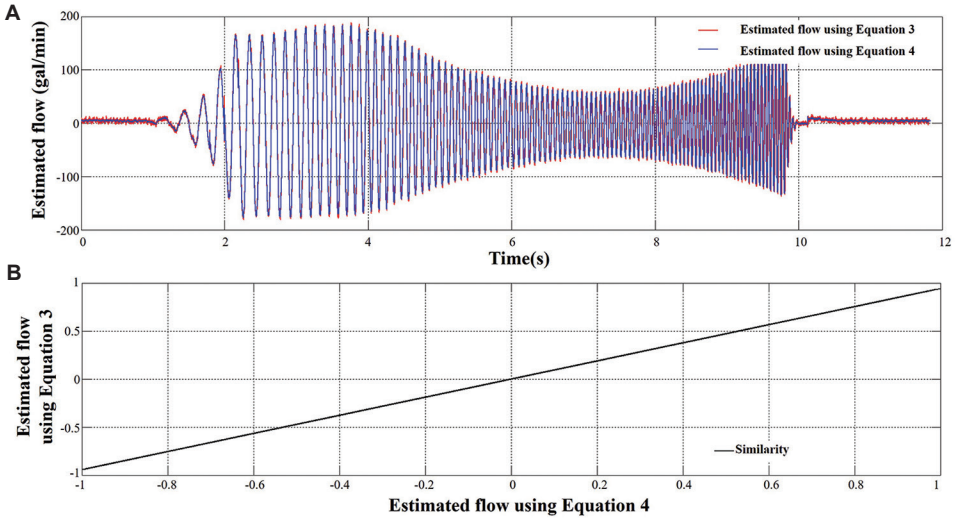

Figure 10. Estimated (A) vibrator oil flow and (B) comparison of flow similarity using **Equations 3** and **4**

shown in Figure 10B. The flow samples estimated using **Equation 4** were assigned to the x-coordinate, while the flow samples estimated using **Equation 3** were assigned to the *y*-coordinate. Together, they form ordered pairs (x, y) that locate points on a coordinate plane.

Theoretically, if the similarity line appears as an oblique line, the data samples in the *x*-coordinate are in-phase with those in the *y*-coordinate, and the two datasets are similar. If the similarity line has a 45° inclination, the data samples in the *x*-coordinate match perfectly with those in the *y*-coordinate in both amplitude and phase.

Figure 10B shows a very strong similarity between the flow curves estimated using **Equations 3** and **4**, although a slight amplitude difference is observed. This amplitude discrepancy is clearly visible near the ordered pairs of (1, 1) and (−1, −1) and is approximately 5%. **Equation 4** provides a method to estimate the vibrator oil flow for any sweep; however, this estimation requires multiple measurements that cannot be obtained during field production. In vibroseis acquisition operations, no pressure sensors are installed; therefore, the supply pressure and the differential pressure are not measured.

In summary, for the estimation of the vibrator oil flow, the two estimation methods based on **Equations 3** and **4** produce highly similar flow curves. This similarity implies that both estimation methods provide reasonable estimates

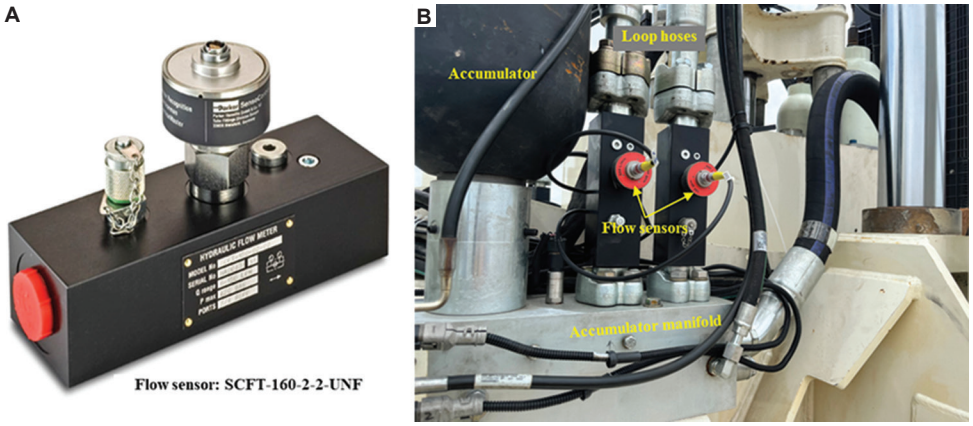

Figure 11. Flow sensor used in the experimental test: (A) sensor model and (B) installation of the flow sensors on the vibrator

of the vibrator oil flow. The two approaches cross-validate each other, demonstrating that each is capable of producing a valid flow estimation.

Based on Figure 10A, the estimated flow approaches the pump maximum capacity of 167 gallons/min between 2 s and 4 s, corresponding to the frequency range from 5 Hz to 9 Hz. Outside this frequency range, the flow demand decreases as the vibrator operates.

For vibrator QC, during the reference or pilot sweep, the reaction mass and baseplate accelerations were measured and recorded for each vibrator sweep. Therefore, the oil-flow estimation method using **Equation 3** is practical for field QC, and its estimated result, as shown in Figure 10, is considered reliable.

3.2. Additional tests for flow estimation verification

To further test the validity of the flow estimation using **Equation 3**, a field test was performed on a vibrator in the Middle East desert. In this test, two flow sensors were successfully installed on the accumulator manifold, enabling direct measurement of the vibrator oil flow.

Figure 11 illustrates the flow sensor model (Figure 11A) used in the experimental test and its installation on the vibrator (Figure 11B). This type of flow sensor can measure flows of up to 160 gallons/min with minimal flow resistance. One side of the flow sensors was installed on the accumulator manifold, and the other side was connected to the loop hoses leading directly to the main-stage servo-valve.

The vibrator performed a linear sweep from 1 Hz to 11 Hz in 20 s at 70% force level, with the sweep frequency increasing linearly at a slow sweep rate of 0.5 Hz/s. This slow sweep rate allowed the vibrator to operate in a steady state, enabling accurate measurement of the vibrator oil flow at low frequencies.

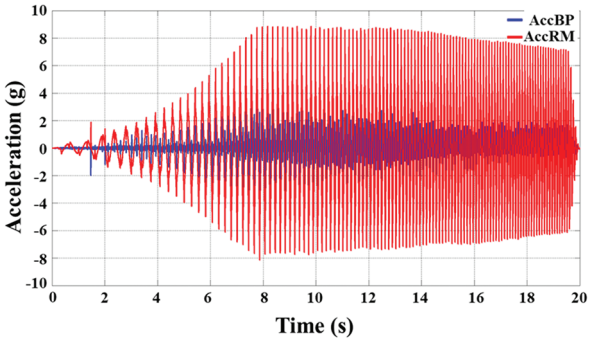

Figure 12. Measured reaction-mass (AccRM) and baseplate (AccBP) accelerations of the vibrator
Abbreviations: AccBP: Accelerations of baseplate; AccRM: Accelerations of reaction mass.

Figure 12 displays a set of measured accelerations of the reaction mass and baseplate. From this set of accelerations, the relative velocity was obtained through an integration operation. Then, the estimated flow was calculated using **Equation 3**. The estimated flow forms a sinusoidal waveform, which is very similar to what is shown in Figure 10A.

For better comparison, a processing algorithm was applied to extract the maximal envelope of the estimated flow. This maximal envelope of the estimated vibrator oil flow is illustrated in Figure 13. For comparison, the measured vibrator oil flow, as shown in Figure 13, was obtained from the raw measured data and smoothed to remove high-frequency spiky noise. In general, the estimated vibrator flow using **Equation 3** agrees well with the measured vibrator flow, although some discrepancies remain.

The estimated flow curve reaches its peak value of 152 gallons/min at 7.9 s, corresponding to a frequency of 5 Hz, while the measured flow reaches its peak value of

155 gallons/min at 8.5 s, corresponding to a frequency of 5.25 Hz. Figure 13 demonstrates that **Equation 3** can be used to estimate the actual vibrator oil flow.

To demonstrate the generalizability of these findings, the estimated flow method based on **Equation 3** was applied in production, where the vibrator operated on the sandy ground surface. This ground surface is a mixture of loose sand and gravel, and it is poorly consolidated. Figure 14 shows an example illustrating the production use of the estimated method based on **Equation 3**. In this case, a low-dwell sweep from 1.5 Hz to 96 Hz in 12 s was applied to shake the AHV-IV 364 vibrator.

Figure 14A illustrates the vibrator ground force, Figure 14B shows the accelerations of the reaction mass and baseplate, and Figure 14C shows the vibrator oil flow estimated using **Equation 3**. It can be observed that the estimated vibrator oil flow is severely asymmetrical.

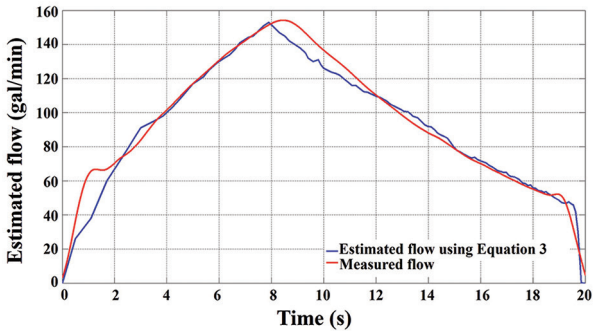

Figure 13. Comparison of estimated and measured vibrator oil flow

Between 4 s and 5 s, corresponding to a frequency range from 5 Hz to 7 Hz, the vibrator flow reaches its maximum with a peak-to-peak value of 250 gallons/min. This indicates that the average flow usage is 125 gallons/min, lower than the maximal pump flow limit of 164 gallons/min.

The estimated vibrator flow curve in Figure 14 provides a QC indication that this low-dwell sweep is compatible with the vibrator hydraulic system, and the vibrator hydraulic system components remain within a safe range. This gentle usage of vibrator oil flow results in no spiky noise in the vibrator ground force, especially at approximately 5 s, when the sweep amplitude changes from the non-linear portion (<5 s) to the linear portion (>5 s), as shown in Figure 14A. With such smooth low-frequency force, less noisy seismic records (Figure 15) are obtained. In addition, the estimated vibrator oil flow can help evaluate the low-frequency sweep design, allowing an optimal low-frequency sweep to be achieved.

4. Discussion

The theoretical framework of this study addresses an unmet need in low-frequency seismic vibrator performance monitoring by proposing methods to estimate vibrator oil flow, which is crucial for QC in seismic data acquisition. The validation of these methods through experimental tests on an AHV-IV 362 vibrator demonstrates good agreement with measurements. The consistency between the estimated and measured oil flows confirms the validity of the theoretical model, highlighting its potential for practical application. This

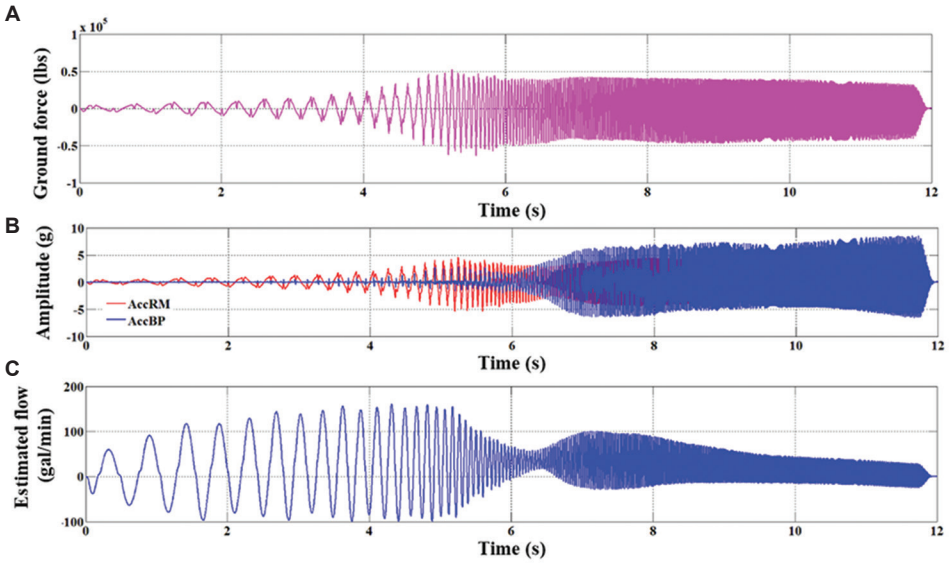

Figure 14. Estimated vibrator oil flow on an AHV-IV 364 vibrator. (A) Vibrator ground force. (B) The accelerations of the reaction mass (AccRM) and baseplate (AccBP). (C) Estimated vibrator oil flow.
Abbreviations: AccBP: Accelerations of baseplate; AccRM: Accelerations of reaction mass.

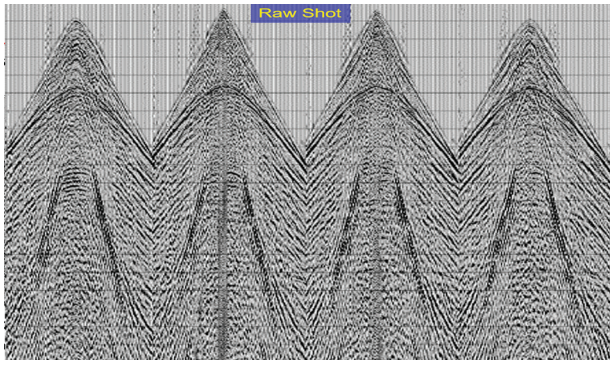

Figure 15. Normal shot records

validation is further supported by tests on an AHV-IV 364 vibrator, reinforcing the methods' robustness across different vibrator models.

Although some discrepancies remain between the two sets of results, they exhibit high consistency, and the level of precision is sufficient to meet production requirements. This demonstrates that the proposed method is theoretically sound and practically feasible. However, it is important to acknowledge certain limitations, such as reliance on sensor accuracy and assumptions embedded in the model. Further refinement and validation under more diverse conditions should be conducted to enhance the robustness and generalizability of the method.

5. Conclusion

Low-frequency vibroseis acquisition has become a routine practice in land seismic operations. At low frequencies, the limitations of vibrator mechanical and hydraulic systems on ground force output are well recognized. During a vibrator low-dwell sweeping, the travel distance of the reaction mass is recorded and monitored. The reaction mass displacement is incorporated into vibrator QC. However, the vibrator oil flow is not measured and, therefore, is not included in vibrator QC. The methods presented in this paper provide an estimation of the vibrator oil flow, enabling real-time QC of the vibrator oil flow. Major failures in vibrator hydraulic system components, such as pilot servo-valves, can be avoided, thereby maintaining high acquisition productivity. Furthermore, the estimated vibrator oil flow can help derive a more practical vibrator force profile at low frequencies, thereby optimizing the low dwell sweep design.

Acknowledgments

We thank BGP for providing the seismic data used in this study and granting permission for the data to be published.

Funding

This study was financially supported by the science and technology project "Research on Multi-physical Field High-Precision Oil and Gas Geophysical Exploration Technology and Equipment" (No.2023ZZ05) of the China National Petroleum Corporation, titled *Theory, Key Technologies,* and *Core Equipment of Full Wave Field Seismic Acquisition*.

Conflict of interest

The authors declare that they have no competing interests.

Author contributions

Conceptualization: Mingtao Nie, Zhouhong Wei
Formal analysis: Mingtao Nie, Zhouhong Wei, Yang Liu
Funding acquisition: Mingtao Nie,Yongfei Qi
Investigation: Tao Fang, Xiaolong Jiang, Yongan Xu
Methodology: Mingtao Nie, Zhouhong Wei
Validation: Zhouhong Wei, Yang Liu
Writing–original draft: Mingtao Nie, Zhouhong Wei, Yongfei Qi
Writing–review and *editing:* All authors

Availability of data

All data analyzed are presented in the paper.

References

1. Rozemond HJ. Slip-Sweep Acquisition. In: *66th Annual International Meeting*. SEG Expanded Abstracts; 1996. p. 64-67.

   doi: 10.1190/1.1826730

2. Allen KP, Johnson ML, May JS. High Fidelity Vibratory Seismic (HFVS) Method for Acquiring Seismic Data. In: *68th Annual International Meeting*. SEG Expanded Abstracts; 1998. p. 140-143.

   doi: 10.1190/1.1820171

3. Bouska J. *Distance Separated Simultaneous Sweeping: The World's Fastest Vibroseis Technique. EAGE Vibroseis Workshop*. Prague, Czech Republic, Extended Abstract; 2008. p. 15983.

4. Howe D, Foster M, Allen A, Jack I, Taylor B. Independent Simultaneous Sources: A Method to Increase Productivity of Land Seismic Crews. In: *78th Annual International Meeting*. SEG Expanded Abstracts; 2008. p. 2826-2830.

5. Wei Z. Design of a P-wave seismic vibrator with advanced performance. *GeoArabia*. 2008;13:123-136.

   doi: 10.2113/geoarabia1302123

6. Wei Z, Hall MA, Phillips TF. Geophysical benefits from an improved seismic vibrator. *Geophys Prospect*. 2012;60:466-479.

doi: 10.1111/j.1365-2478.2011.01008.x

7. Wei Z, Criss J, Wang R, Clow A. A new generation low-frequency seismic vibrator. *Geophysics*. 2022;87(4):P29-P38.

   doi: 10.1190/geo2022-0010.1

8. Peng X, Sun J, Li Y, Teng Z, Hao L. Modeling and analysis of a shear-wave vibrator-ground coupled system dynamics. *Int J Mech Sci*. 2025;289:110064.

   doi: 10.1016/j.ijmecsci.2025.110064

9. Rowse SL, Heath B. The vibrator and its interaction with the ground. *First Break*. 2025;43(1):75-81.

   doi: 10.3997/1365-2397.fb2025007

10. Robin A, Secker S. Source Motion Corrections for Marine Vibrator Data: Who's Who and What They're Not. In: *86th EAGE Annual Conference* and *Exhibition*. Vol. 1. European Association of Geoscientists and Engineers; 2025. p. 1-5.

11. Xiao Y. Nonlinear sweeping signal design of vibrator based on spectral characteristics. *Progress in Geophysics*. 2021;36(1):300-309. [Article in Chinese].

    doi: 10.6038/pg2021ee0127

12. Wei T, Zhu Y, Liu Z,Wang D, Wei G, Nie M. Design of Low Frequency Sweep Signals for Conventional Vibrators. In: *SEG International Exposition* and *Annual Meeting*. SEG; 2024. p. 4090586.

    doi: 10.1190/image2024-4090586.1

13. Qi YF, Wei ZH, Nie MT, *et al*. Low-frequency sweep design-a case study in middle east desert environments. *Appl Geophys*. 2024;22(1):71-83.

    doi: 10.1007/s11770-024-1126-3

14. Liu Y, Wen X, Li B, An Z, Wu D. Designing nonlinear sweep signal to improve the resolution of vibroseis acquisition. *Geophysics*. 2025;90(5):P73-P86.

    doi: 10.1190/geo2024-0490.1

15. Sallas JJ. How do hydraulic vibrators work? A look inside the black box. *Geophys Prospect*. 2010;58(1):3-18.

    doi: 10.1111/j.1365-2478.2009.00837.x

16. Sallas JJ. Seismic vibrator control and the downgoing P-wave. *Geophysics*. 1984;49:732-740.

    doi: 10.1190/1.1441701

17. Mahrooqi S, Rawahi S, Yarubi S, *et al*. Land Seismic Low Frequencies: Acquisition, Processing and Full Wave Inversion of 1.5-86 Hz. In: *82nd Annual International Meeting*, *SEG Exp*and*ed Abstracts*; 2012.

    doi: 10.1190/segam2012-0961.1

18. Wei Z. Pushing the vibrator ground-force envelope towards low frequencies. *Geophys Prospect*. 2009;57(1):151-161.

    doi: 10.1111/j.1365- 2478.2008.00738.x

19. Wei Z. A new generation low frequency seismic vibrator. In: *85th Annual International Meeting*. SEG Expanded Abstracts; 2015. p. 211-215.

    doi: 10.1190/segam2015-5713173.1

20. Wei Z, Criss J, Bull A, Liang F, Wu Y. The low-frequency seismic vibrator: Design and experimental verification. *First Break*. 2018;36(1):77-84.

    doi: 10.3997/1365-2397.n0066

21. Bagaini C, Dean T, Quigley J, Tite G, Inventors. Westerngeco LLC, Assignee. *Systems and Methods for Enhancing Low-Frequency Content in Vibroseis Acquisition*. US Patent US 7,327,633 B2. 2008.

22. Phillips TF, Wei Z, Inventors. INOVA LTD., Assignee. *Seismic Frequency Sweep Enhancement*. US Patent US 9,121,961 B2. 2015.

23. Sallas JJ, Inventors. CGG VERITAS, Assignee. *System and Method for Determining a Frequency Sweep for Seismic Analysis.* US Patent US 9,535,178 B2. 2017.

24. Dellinger JA, Harper M, Inventors. BP Corporation North America Inc., Assignee. Harper M. *System and Method for Performing Seismic Surveys with a Controlled Source using Maximum-Power Sweeps* . US Patent US 9,702,991 B2. 2017.

25. Merritt HE. *Hydraulic Control Systems*. United States: John Wiley and Sons, Inc.; 1967.